J Mater Sci: Mater Med (2011) 22:2097–2109
DOI 10.1007/s10856-011-4385-5

Delivery of chemotropic proteins and improvement of dopaminergic neuron outgrowth through a thixotropic hybrid nano-gel

Elisa Tamariz · Andrew C. A. Wan · Y. Shona Pek · Magda Giordano · Genoveva Hernández-Padrón · Alfredo Varela-Echavarría · Iván Velasco · Víctor M. Castaño

Received: 19 January 2011 / Accepted: 25 June 2011 / Published online: 9 July 2011
© Springer Science+Business Media, LLC 2011

Abstract Chemotropic proteins guide neuronal projections to their final target during embryo development and are useful to guide axons of neurons used in transplantation therapies. Site-specific delivery of the proteins however is needed for their application in the brain to avoid degradation and pleiotropic affects. In the present study we report the use of Poly (ethylene glycol)-Silica (PEG-Si) nanocomposite gel with thixotropic properties that make it injectable and suitable for delivery of the chemotropic protein semaphorin 3A. PEG-Si gel forms a functional gradient of semaphorin that enhances axon outgrowth of dopaminergic neurons from rat embryos or differentiated from stem cells in culture. It is not cytotoxic and its properties allowed its injection into the striatum without inflammatory response in the short term. Long term implantation however led to an increase in macrophages and glial cells. The inflammatory response could have resulted from non-degraded silica particles, as observed in biodegradation assays.

E. Tamariz (✉)
Instituto de Ciencias de la Salud, Universidad Veracruzana, Av. Luis Castelazo Ayala s/n, 91190 Xalapa, VER, México
e-mail: elisatammx@gmail.com; etamariz@uv.mx

A. C. A. Wan · Y. S. Pek
Institute of Bioengineering and Nanotechnology, 31 Biopolis Way, The Nanos 138669, Singapore

M. Giordano · A. Varela-Echavarría
Instituto de Neurobiología, Universidad Nacional Autónoma de México, Blvd. Juriquilla 3001, 76230 Querétaro, QRO, México

G. Hernández-Padrón · V. M. Castaño
Centro de Física Aplicada y Tecnología Avanzada, Universidad Nacional Autónoma de México, Blvd. Juriquilla 3001, 76230 Querétaro, QRO, México

I. Velasco
Instituto de Fisiología Celular-Neurociencias, Universidad Nacional Autónoma de México, 04510 México, DF, México

1 Introduction

Site-specific delivery of growth factors and other diffusible molecules in the Central Nervous System (CNS) is a challenging enterprise, due to the need to protect them from degradation, thus avoiding pleiotropic effects, while doing so through a minimally invasive and non-damaging method. The use of transplanted cells, viral vectors, or artificial devices, such as pumps and catheters for in situ protein delivery to the CNS leads to several problems such as inflammatory response, over expression, uncontrolled cell transformation and growth, highly invasive procedures, malfunction and infections [1–3]. The use of polymeric biomaterials for delivery of neurotransmitters or neurotrophic factors in the form of microparticles [4–6], nanoparticles [7] or injectable hydrogels [8–11] into the CNS has been shown to be a feasible alternative. Delivery of injectable polymers is particularly advantageous for applications that require a well defined physical space and specific delivery with a low invasive method, such as stereotaxic surgery. Polymeric release systems include those in which the drug is bound to the polymer either chemically or via affinity interactions, and those in which the drugs are physically encapsulated. Due to the simplicity of the latter and to the fact that drugs are minimally exposed to harsh conditions, physical encapsulation in injectable polymers provides an appealing alternative for site-specific drug and growth factor delivery in the brain [2, 12].

Chemotropic proteins are mainly expressed during development of the CNS and are involved in the

stereotypical projection of axons to establish the neuronal connections. Chemotropic proteins exert their function through the formation of gradients. The growth cones of neurons detect small concentration changes across the spatial span, and the magnitude and shape of the gradients influence the growth cone, depending of the neuronal type [13–15]. The lack of a concentration gradient or a similar increase in concentration of the chemotropic proteins induces the stop of axonal projections in retinal ganglionar neurons, cortical and Til neurons respectively [14–16]. Semaphorins (sema) are a family of chemotropic glycoproteins with a characteristic extracellular domain of 500 amino acids [17]. Class 3 semaphorins are secreted proteins and are mainly known for their repulsive effects on neurites [18]. During development, repulsive effects of sema 3A on the dorsal root ganglion neurons (DRG) helps to target the nociceptive sensory DRG axons to the dorsal root of the spinal cord [19]. Sema 3A, however, also exerts attractive effects on other neurons like cerebellar and cortical neurons [20, 21], and dopaminergic neurons of the ventral mesencephalon [22]. In spite of the considerable knowledge of semaphorin signaling, the factors that influence attractive or repulsive effects are still under study. Dual action of semaphorins of class 3 depend not only on the affinity to the heterodimeric transmembrane receptor of neuropilin and plexin proteins [23], but also on intracellular contexts like cyclic nucleotides concentration [24, 25], the interaction with adhesion molecules of the immunoglobulin superfamily (IgCAMs) like L1 [26], or the engagement of integrin receptors to the extracellular matrix [27, 28]. Class 3 semaphorins have been implicated in the guidance of axons of dopaminergic (DA) neurons during the formation of the nigrostriatal pathway (NP) [22]. NP is a dopaminergic projection from the ventral midbrain to striatum at the telencephalon, and it is involved in motor and cognitive tasks; its degeneration in humans leads to the symptoms of Parkinson's Disease (PD). It has been observed that sema 3A and 3C enhance axon outgrowth and that sema 3C also attracts the axons of dissociated DA neurons obtained from rat embryos, or by the differentiation of embryonic stem cells, thus suggesting their use in directing and enhancing the outgrowth of transplanted DA neurons for cell replacement therapies of PD [29]. One major challenge in neuronal replacement therapies is the correct projection and innervation of the transplanted cells in the host brain to reconstruct the degenerated neuronal pathways [30–35], therefore the use of sema could be useful for the guidance and enhancement of axonal outgrowth. Delivery of semaphorins at the final target or near the intranigral transplanted neurons however, would be necessary to form a gradient and to guide the projections of the transplanted cells.

Accordingly, in this paper we report the use of a novel thixotropic hybrid poly (ethylene glycol)-silica (PEG-Si) nano-gel for establishing a chemotropic gradient that could be used to guide axons of grafted DA neurons. The PEG-Si nano-gel is formed of aggregated nanoparticles, where the PEG and silica phases are homogenously dispersed and chemically interacting, so as to form a truly hybrid organic–inorganic material. The weak association between the particles is disrupted by moderate shear force that liquefies the gel state [36], making it suitable for inclusion of proteins and injection into the CNS. Our results show that PEG-Si is able to deliver a functional sema 3A and to form a gradient of concentration without in vitro cytotoxic effects. In vivo experiments showed that it is suitable for CNS injection, as well. However, a late onset inflammatory response was observed that could be caused by the biodegradation products.

2 Materials and methods

2.1 Diffusion of proteins

To measure the diffusion of proteins included in the PEG-Si nano-gel, Mouse IgG coupled to Alexa 488 (Invitrogen, Carlsbad CA) was mixed with the polymer at a final concentration of 80 ng/µl, a drop of 2 µl was added to a microscope slide and polymerized for 10 min at 37°C. After polymerization, 35 µl of a rat tail collagen solution was added to the PEG-Si nano-gel, maintaining the drop of the polymer on one side of the collagen gel, and polymerized for 40 min at 37°C (Time 0). To measure the diffusion of fluorescent immunoglobulins into the collagen matrix, the gels were mounted with a coverslip at several time points and observed under an epifluorescent microscope (Olympus, Center Valley PA). Micrographs of the fluorescent images and their equivalent phase contrast images were obtained to register all the gel area, and reconstructed images were obtained using Photoshop CS2 software (Adobe Systems, San Jose, CA). Fluorescent signals were measured by obtaining the optical density trough a traced area in the collagen gel image that comprised from the more proximal area of the PEG-Si gel to the more distal zone of it, using the Image Pro Plus software (Media Cybernetics, Inc., Bethesda, MD). Calibration of the intensity parameters was done as follows: 0% of intensity was calibrated at an area where no collagen gel was present, 100% of intensity was calibrated at the center of the PEG-Si gel.

To measure the diffusion of proteins in the culture medium, PEG-Si gels containing 80 ng/µl of IgG Alexa488 and included in a collagen gel as mentioned before, were incubated at 37°C with Optimem (Invitrogen). The culture

medium was collected at several time points and the fluorescent intensity of each sample medium was measured immediately with a luminometer coupled to a fluorescent module (Turner BioSystems Inc. Sunnyvale CA). As a positive control, Optimem medium plus IgG coupled to Alexa 488 (80 ng/μl) was incubated at 37°C for the same period of time as the collagen gels and the fluorescence signal was measured as previously described.

2.2 DRG culture and collapse assay

DRGs were obtained from E14 rat embryos and cultured over a poly-L-ornithine (Sigma, St Louis MO)-treated coverslip incubated with laminin (0.01 mg/ml) (BD biosciences, Franklin Lakes NJ). DRG explants were incubated for 24 h to allow axonal outgrowth in basal medium as described previously [37], plus 15 ng/ml of NGF (Invitrogen). For the collapse assay explants were pre-incubated for 40 min with basal medium plus 5 ng/ml of NGF, and after the incubation a drop of 2 μl of PEG-Si nano-gel containing the recombinant sema 3A-Fc (R&D Biosystems, Minneapolis MN) (0.5 μg/ml) or recombinant IgG-Fc (R&D Biosystems) (0.5 μg/ml) was added near them. Growth cone collapse effects were recorded under phase contrast inverted microscope (Olympus) by obtaining micrographs every 15 min. The percentage of collapsed growth cones was calculated in the proximal and distal area to the PEG-Si gel as shown in Fig. 2f, using images obtained by confocal microscopy of cultures previously incubated for 30 min with rhodamine phalloidin (Sigma), and the differences between means were calculated using the Student's *t*-test ($P < 0.05$).

2.3 Culture of dopaminergic neurons

Ventral mesencephalic explants of E14 rat embryos were obtained in Hank's solution (Invitrogen) and partially disaggregated as described previously [22]. The cells were resuspended in a rat tail liquid collagen mix at a proportion of 0.5 explants per 35 μl of collagen. The mix of collagen plus the neurons was poured into a 24 well tissue culture plate where a 2 μl drop of PEG-Si nano-gel had been previously polymerized. After 40 min of polymerization at 37°C and 5% CO_2, 350 μl of culture medium containing 50% DMEM-F12 (Invitrogen), 50% DMEM (Invitrogen), 1.5% glucose, B-27 supplement (Invitrogen) and 1% penicillin- streptomycin (Invitrogen) was added to each well. Differentiated dopaminergic neurons were obtained as follows; R1 ES cells were differentiated using the five stage protocol as previously reported [38]. Briefly undifferentiated ES cells were seeded on bacterial culture dishes to form embryoid bodies. Embryoid bodies were transferred to a tissue culture plate and incubated for 7–11 days with serum-free medium supplemented with insulin, transferrin, selenite and fibronectin (ITSFn) to select nestin precursor cells. Nestin populations were expanded with N2 medium (Invitrogen) supplemented with FGF2 (Peprotech, Rocky Hill, NJ), FGF8b (Peprotech) and Shh (R&D Biosystems) for 4–6 days. Final differentiation was induced by incubation with N2 medium supplemented with ascorbic acid (Sigma).

2.4 Cytotoxicity assay

Collagen gel cultures containing dissociated dopaminergic neurons exposed to PEG-Si polymer were incubated for 2 or 8 days without changing the culture medium. Gels were washed with Optimem medium (Invitrogen) and incubated in a mix of Calcein AM and Ethidium homodimer-1 according to the manufacturer instructions (Invitrogen). After incubation gels were washed 2 times with PBS, mounted on a slide and observed under an epifluorescent microscope. Ten fields per gel ($n = 3$) were recorded on micrographs and the percentage of live (green) versus dead (red) cells was obtained. Differences between means of control and PEG-Si gel exposed cultures were statistically analyzed using Student's *t*-test ($P < 0.05$).

2.5 In vivo injection of PEG-Silica polymer

Adult Wistar rats were anesthetized using a mix of Ketamine-Xylazine (70 mg/kg–6 mg/kg). All the surgical procedures were performed under aseptic conditions. The skull was exposed and a hole was drilled using a high speed dental drill. Bilateral stereotaxic injections were performed into the center of the striatum using a Hamilton micro syringe coupled to a 21-gauge needle. The coordinates were: 0.7 mm anterior posterior from Bregma, 2.8 mm mediolateral from Bregma and 4.0 mm from the cortical surface. Right hemispheres were injected with sterile saline solution and left hemispheres with UV irradiated PEG-Si nano-gel, previously liquefied by vigorous shaking. After the needle reached the striatum it was left to equilibrate for 5 min, 3 or 5 μl of saline solution or PEG-Si were slowly injected (about 5 min), and the needle was slowly removed after being left inside for three additional minutes. The wound was sutured and the animals were left to recover from the anesthesia under a lamp to avoid hypothermia. Animals were kept in their home-cages with free access to food and water until the day of euthanasia. All the procedures were performed in accordance with the regulation of Mexican government regarding the use of laboratory animals for research purpose (NOM-062-ZOO-1999), and following the guide for the Care and Use of Laboratory Animals of the Institute of Laboratory Animal Resources, U.S. National Research Council (1996).

2.6 Immunostaining

Collagen gels previously fixed with 3.5% paraformaldehyde (PFA) were incubated with rabbit anti-TH antibody (Pel-Freez, Rogers, AK) as previously described [22, 29]. Brains obtained after transcardial perfusion with PBS and 4% PFA were post fixed overnight with the same fixative, extensively washed with PBS and cryoprotected using Tissue-Tek O.C.T. compound. 20 μm cryostat serial sections were obtained and mounted on slides. Slides were washed with PBS, pre-incubated with 5% goat serum in PBS, and incubated overnight with antibodies against activated macrophages (ED-1) (Millipore) and/or GFAP (Millipore). Slides were extensively washed with PBS and incubated with the appropriate secondary antibody (anti-rabbit or anti mouse IgG coupled to Alexa 488 or Alexa 546; Invitrogen). Slides were mounted using anti-fade mounting medium and observed under confocal microscopy (Zeiss, LSM510). Panoramic images of the sections were obtained using Photoshop CS2.

2.7 Raman spectroscopy

PEG-Si samples were incubated in SBF [39] for different lengths of time at 37°C and 5% of CO_2. Overnight dried samples were measured in a Raman microspectrometer (Senterra Bruker, Billerica MA), equipped with an Ar laser emitting at 760 nm, coupled with an Olympus Bx51M microscope with a 20× objective, at 100 mW, 10 s of time integrated and 6 scans. All measurements were carried out at room temperature with no special sample preparation.

3 Results

3.1 PEG-Silica thixotropic nano-gel is suitable for protein diffusion and formation of a protein gradient in collagen matrices

Chemotropic proteins exert either an attractive or repulsive effect by a concentration gradient that is sensed by the axonal growth cone. To evaluate the diffusion rate of proteins included in a PEG-Si nano-gel and the ability to form a concentration gradient of a protein in an extracellular matrix such as collagen, immunoglobulins coupled to the fluorophore Alexa 488 were included in a PEG-Si polymer and a 2 μl drop of the mix was included in a 35 μl drop of collagen solution (Fig. 1a). After 40 min of polymerization (time 0), the diffusion of the fluorescent signal was observed at different time-points under an epifluorescent microscope, the intensity of the fluorescence was calculated based on the optical density of the images, and expressed as percentage of the fluorescent observed at the center of the PEG-Si gel (Fig. 1b). A gradual diffusion of fluorescence through the collagen gel was observed, indicating the formation of a concentration gradient of the protein (Fig. 1c). Two hours after incubation, 69% of the fluorescent signal was detected adjacent to the PEG-Si nano-gel and less than 2% at the more distal zone. After 6 h of incubation, the fluorescent signal increased to almost 80% at the area adjacent to the PEG-Si nano-gel, and about 20% at the more distal part of the collagen gel (Fig. 1b, c). A full day later, the gradient of proteins was still detectable but became less pronounced than that observed at 6 h (Fig. 1b, c). The fluorescent immunoglobulins contained in the collagen gel did not diffuse outside the collagen matrix, since no fluorescent signal was observed in the culture media, as compared to the fluorescent signal obtained in the media when the immunoglobulins were directly added to it (Fig. 1d). These results show that proteins included in a PEG-Si nano-gel can form a concentration gradient within an extracellular matrix like a collagen gel.

3.2 Recombinant Semaphorin 3A included in a PEG-Silica nano-gel exerts a repulsive effect on axons of dorsal root ganglion neurons

Sema 3A is a chemotropic protein originally described to induce the collapse of axonal growth cones of dorsal root ganglion (DRG) neurons [40]. To evaluate whether the inclusion of recombinant sema 3A (sema3A-Fc) in a PEG-Si nano-gel has the previously described collapse effect on DRG neurons, we cultured DRG explants obtained from rat embryos at the development stage (E) 14, adjacent to a drop of PEG-Si plus 0.5 μg/ml of sema 3A-Fc, or PEG-Si nano-gel plus 0.5 μg/ml of recombinant IgG immunoglobulin (IgG-Fc), as a control. The growth cone morphology of DRG neurons exposed to the gels was monitored in a phase contrast microscope. After 50 min of incubation, no growth cone collapse was observed when the DRG explants were exposed to the control gel (Fig. 2a, b). Nevertheless, exposure of DRG explants to the sema 3A-Fc containing gels induced the collapse of the growth cones (Fig. 2c, d). More growth cone collapse was observed on the proximal quadrant than on the distal quadrant of the explants (Fig. 2f). To quantify the differences in growth cone collapse between the proximal and distal quadrants of the DRG explants, cultures exposed to sema-3A-Fc gel or control gel were fixed and the actin fibers were labeled with rhodamine-phalloidin to visualize the growth cones by confocal microscopy (Fig. 2g, h). A higher percentage of collapsed growth cones was observed at the side facing the gel containing sema 3A-Fc as compared to the side facing away from it. No difference in growth cone collapse was observed between the proximal and distal quadrants of the explants in control gel-exposed cultures (Fig. 2i). These results show that recombinant

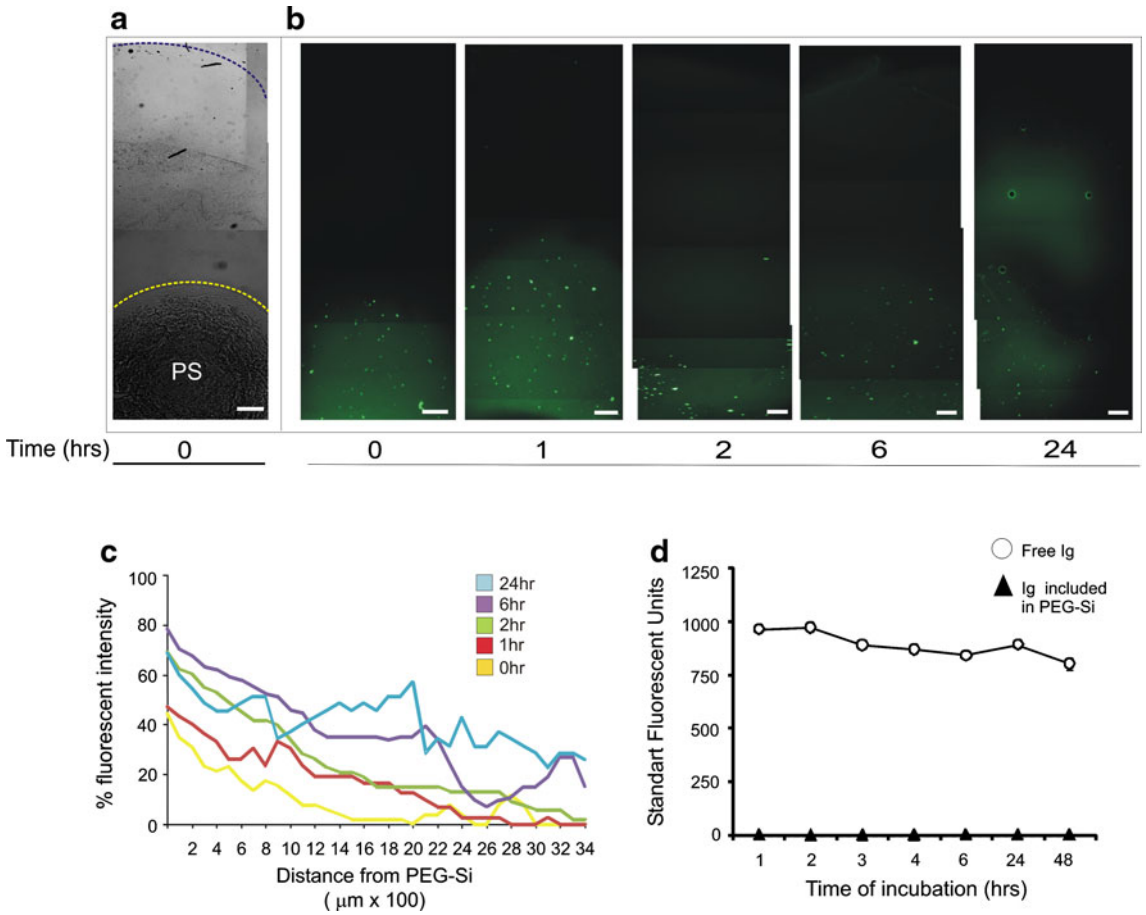

Fig. 1 Diffusion of fluorescent protein included in a PEG-Si nano-gel and gradient formation in a collagen gel. Immunoglobulins coupled to Alexa 488 were mixed with the PEG-Si nano-gel to a final concentration of 80 ng/µl, 2 µl drops of the mix were polymerized and included in 35 µl of collagen solution which was polymerized for 40 min at 37°C (Time 0). The diffusion of the fluorescent protein was registered with an epifluorescence microscope at 0, 1, 2, 6, and 24 h. **a** Light interference microscopy reconstructed image of the PEG-Si nano-gel (PS) (delimited by *yellow dotted lines*) included in a collagen gel (delimited by *blue dotted lines*) at time 0. **b** Epifluorescence microscopy reconstructed images of collagen gels with fluorescent immunoglobulins at different times of incubation. **c** Fluorescence intensity distribution in the collagen gels from the area adjacent to the PEG-Si nano-gel to the more distal area at different times of incubation. **d** Fluorescent signal of IgG-Alexa 488 in the culture media when directly added to medium (*circles*), or included in a PEG-Si nano-gel plus collagen gel (*triangles*). $n = 3$. *Scales bars* in **a** and **b** 500 µm

sema 3A included in a PEG-Si nano-gel maintains its collapse-inducing activity and diffuse gradually in the culture media, being more effective on the proximal section of the explants.

3.3 Recombinant sema 3A included in a PEG-Silica nano-gel increases axonal outgrowth of dopaminergic neurons obtained from embryonic ventral mesencephalon or from differentiated embryonic stem cells

To evaluate whether recombinant sema 3A included in a PEG-Si gel could exert its previously reported attractive effect on dopaminergic neurons [29], disaggregated ventral mesencephalic dopaminergic neurons (mDA) from E14 rat embryos were included in collagen gels, together with a 2 µl drops of PEG-Si nano-gel containing different concentrations of sema 3A-Fc or control IgG-Fc. After 48 h in culture, the dopaminergic neurons were detected by immunostaining with an anti-tyrosine hydroxylase (TH) antibody. Axonal outgrowth of immunostained neurons was measured from confocal images. An increase of 53 and 68% in dopaminergic axon outgrowth was observed when neurons were exposed to PEG-Si with 2 µg/ml (Fig. 3b, c) or with 5 µg/ml (Fig. 3e, f) of sema 3A-Fc, as compared to cultures exposed to equivalent concentrations of IgG-Fc (Fig. 3a, d). No increase in axonal outgrowth was observed when neurons were exposed to 10 µl/ml of sema 3A-Fc (Fig. 3g–i).

Evaluation of the percentage of live and dead mDA neurons in the cultures exposed to PEG-Si nano-gels showed no cytotoxic effect at a time point equivalent to that used to evaluate the effect of sema 3A-Fc (2 days), or

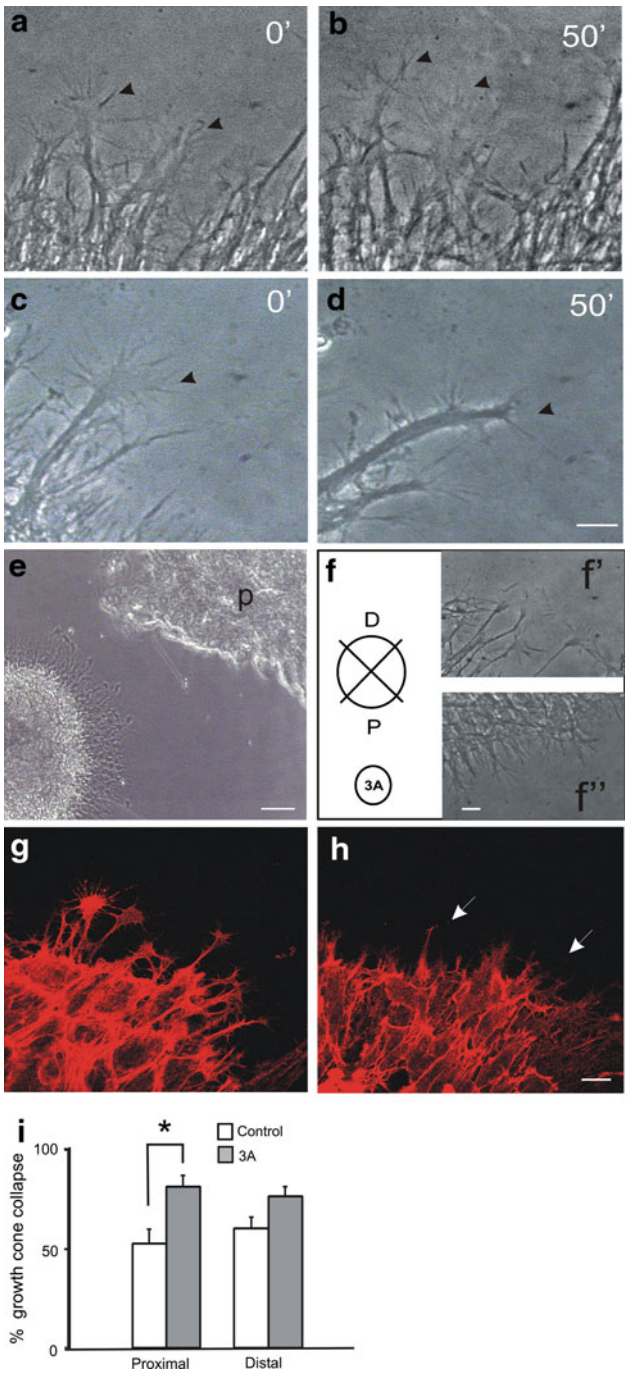

◀ **Fig. 2** Effect of recombinant Semaphorin 3A included in a PEG-Si nano-gel on DRG neurons growth cone collapse. E14 rat embryo dorsal root ganglion explants cultured on laminin-coated coverslips were exposed to PEG-Si gel containing IgG-Fc (**a**, **b**) or PEG-Si gel containing recombinant sema 3A-Fc (**c**, **d**), and phase contrast microscopy images were obtained at 0 min (**a**, **c**) or 50 min (**b**, **d**) of incubation. No growth cone collapse was observed with the polymer alone, only the movement of the growth cone was observed (**b**, *arrowheads*). A complete collapse of a growth cone is observed in DRG neurons exposed to sema 3A-Fc (**d**, *arrowhead*). (**e**) Phase contrast micrograph at low magnification showing the DRG ganglion exposed to the polymer (p). (**f**) Schematic representation of a DRG explant to show the outgrowth on the quadrants of distal and proximal areas with respect to the sema 3A-Fc containing PEG-Si gel. (**f′**) Phase contrast micrograph of the distal area. (**f″**) Phase contrast micrograph of the proximal area. (**g**) Growth cones of the distal area of sema 3A-Fc treated cultures stained with rhodamine phalloidin. (**h**) Growth cones of the proximal area exposed to sema 3A-Fc and stained with rodhamine phalloidin showing collapsed growth cones (arrows). (i) Graph showing the percentage of collapsed growth cone in distal and proximal areas of DRG explants exposed to polymer with sema 3A-Fc (3A), or without it (control), (*$P = 0.05$, according to Student's *t*-test) ($n = 4$ explants per condition). *Scale bars* in **d** 20 μm and applies to **a**–**c**, **e** 50 μm, **f″** 20 μm and applies to **f′**, **h** 20 μm and applies to **g**

after 8 days of exposure (Fig. 3j). An increase in the percentage of dead neurons was observed in control and PEG-Si treated cultures after 8 days of culture, likely due to the exhaustion of nutrients in the culture medium. When dopaminergic neurons differentiated from embryonic stem cells were exposed to PEG-Si nano-gel containing 2 μg/ml of sema 3A-Fc or an equivalent concentration of an IgG-Fc, 45% increase in axonal length was observed in sema 3A-Fc treated cultures as compared with control cultures (Fig. 4a–c).

3.4 Biocompatibility of PEG-Silica nano-gel in the central nervous system

To evaluate if the PEG-Si nano-gel is an appropriate vehicle to deliver the recombinant sema 3A into the brain, we implanted the polymer into the striatum of adult rats, a potential site for the injection of semaphorins. Bilateral injections of 3 or 5 μl of sterile saline solution in one hemisphere, and the same amount of PEG-Si polymer mixed with fluorescent dextran or with Hoechst dye was performed by stereotaxic surgery. Three, 12 or 30 days after the injection the brains were obtained, cryoprotected, and coronal sections (20 μm) were immunostained with an antibody to detect activated macrophages and microglia (ED-1), and/or with anti GFAP antibody to detect gliosis. Three days after injection, accumulation of macrophages was observed in the cortex and near the pial surface in the clot formed at the entry of the needle (Fig. 5a, b, arrows), both in saline solution and PEG-Si injected hemispheres. ED1 positive cells were also observed at the deepest area of injection in the striatum (Fig. 5e, f), however the recruitment of macrophages was restricted to the injury site in the control and PEG-Si treated tissue. ED-1 positive cells were observed in the PEG-Si nano-gel identified by the fluorescent dextran (Fig. 5c–d, g–h), or by the blue staining of Hoechst (Fig. 5j). GFAP immunostaining showed a small amount of gliosis at the injury site in saline and polymer treated hemispheres (Fig. 5i, k). Twelve days after injection ED-1 cells were still observed limited to the injury site, with a similar appearance in both control and treated hemispheres (Fig. 5l, n). GFAP staining showed accumulation of glial cells mainly in the cortex, near the pial

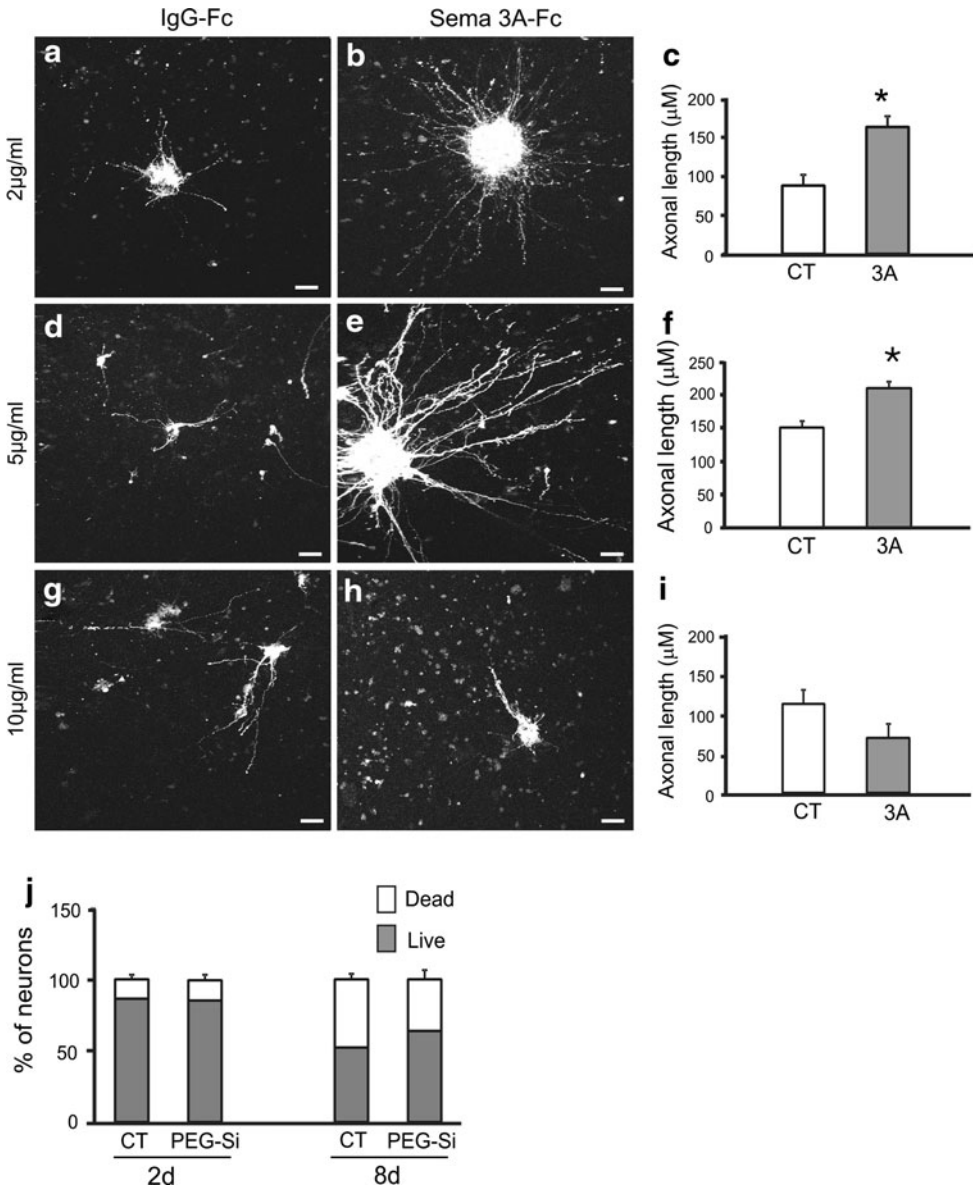

Fig. 3 Recombinant semaphorin 3A included in a PEG-Si nano-gel increase axon outgrowth of ventral mesencephalic dopaminergic neurons. Ventral mesecencephalic dopaminergic neurons obtained from E14 rat embryos were disaggregated and included in a collagen gel containing a PEG-Si nano-gel drop with recombinant human IgG-Fc (control) (**a**, **d**, **g**) or recombinant sema 3A-Fc (**b**, **e**, **h**). (**c**, **f**, **i**) Comparison of the outgrowth of tyrosine hydroxylase-positive (TH^+) axons in cultures with PEG-Si gels plus IgG-Fc (CT) ($n = 4$), or PEG-Si nano-gels plus sema 3A-Fc (3A), at a concentrations of 2 µg/ml (**c**) ($n = 4$), 5 µg/ml (**f**) ($n = 3$), or 10 µg/ml (**i**) ($n = 4$), ($^*P < 0.05$, according to Student's *t*-test). (**j**) Percentage of live and dead neurons present in cultures of partially dissociated embryonic ventral mesencephalons (CT), or in cultures exposed to PEG-Si gels for 2 or 8 days, no differences were observed between the two conditions ($P > 0.05$, according to Student's *t*-test) ($n = 3$ cultures per condition). *Scale bars* 20 µm

surface in both conditions (Fig. 5m, o). After 30 days of injection however, an important increase in the inflammatory response was observed in the polymer injected hemisphere. A wide mass of ED-1 positive cells was detected at the injury site surrounded by GFAP positive cells (Fig. 5r, s); but also outside the area of injection, such as in the choroid plexus in the ventricular area (not shown). GFAP-positive cells were also observed invading the injury site (Fig. 5s). In the control hemisphere ED-1- and GFAP-positive cells were observed only at the injection site in the scar formed at the point of entry of the needle, similar to what was observed at earlier time points (Fig. 5p, q).

The amount of ED1 and GFAP positive cells in the ventral part of the striatum were quantified each 60 µm using the serial sections that included the injury area. Three and twelve days after the stereotaxic injection no differences were observed between polymer and control hemispheres ($P > 0.05$), indicating that the observed inflammatory reaction was mainly due to the wide penetrating lesion. However, 30 days after injection an increase in ED-1- and GFAP-positive cells in the polymer injected hemispheres was observed as compared to saline injected hemispheres ($P < 0.05$) (Fig. 6a).

3.5 Biodegradation of PEG-Silica nano-gel

It was difficult to ascertain if the gel remained in the brain or was degraded in implanted rats, due to the loss of Hoechst staining and the diffusion of fluorescent dextran; however we were able to observe the in vitro degradation

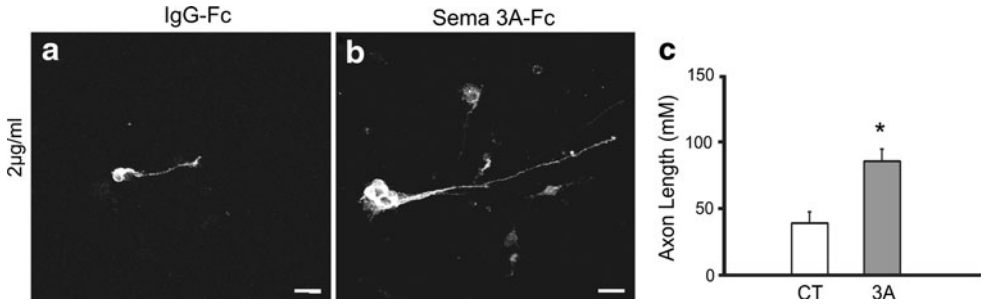

Fig. 4 Recombinant semaphorin 3A included in a PEG-Si nano-gel increase axonal outgrowth of dopaminergic neurons differentiated from embryonic stem cells. Dopaminergic neurons differentiated from embryonic stem cells were disaggregated and included in a collagen gel containing **a** drop of PEG-Si with recombinant human IgG-Fc (**a**), or sema 3A-Fc (**b**). (**c**) Comparison of TH^+ axons lengths between treated (3A) and control (CT) cultures, ($^*P < 0.05$, according to Student's *t*-test) ($n = 3$ gels per condition). *Scale bars* 10 μm

of PEG-Si by incubating it in Simulated Body Fluid (SBF), and by evaluating its biodegradation by Raman scattering spectroscopy at different incubation times. We observed the characteristic absorption bands of the PEG-silica system at 1136 and 1063 and 1043 cm^{-1} corresponding to the C–O–C group, two bands at 2958 to 2883 cm^{-1} within the interval from 3000 to 2800 corresponding to the wide absorption band assignment of the $–H(CH_3)$ group [41], and an absorption corresponding to the vibration of the C–H group at 1470 cm^{-1} [42]. The bands at 3130, 2500 and 486 cm^{-1} corresponded to silica groups within the system. Absorptions due to the salts of the SBF were present at 945 and 760 cm^{-1} [43] (Fig. 6b). We observed PEG-Si sample degradation after the first 24 h of incubation: the band at 1136 cm^{-1} is deformed over time into two bands, this can be appreciated as a hump around 1133 cm^{-1} and it becomes more evident after 72 h of incubation in the absorption bands at 1129 and 1141 cm^{-1} (Fig. 6c, inset). The degradation of $H-(CH_3)$ groups in the interval from 2800 to 2945 cm^{-1} is observed in the formation of the peaks at 2890 and 2950 cm^{-1} (Fig. 6d). In contrast, the silica bands of 2500 cm^{-1} and 3130 cm^{-1} remained unchanged, even after 30 days (Fig. 6d). From these results we concluded that degradation occurs mainly by the interaction of PEG with the salts in the SBF whereas the silica phase remains virtually undegraded.

4 Discussion

Cell replacement therapy for PD using dopaminergic neurons from differentiated stem cells, and more recently from induced pluripotent stem cells, is being actively explored. Several evidences of the advantages of having a practically unlimited source of neurons, and the feasibility to implant them to obtain relief of some of the PD symptoms have been reported [30, 32–35, 44]. However, the ectopic transplantation of neurons into the striatum, outside their endogenous site in the mesencephalon, has shown limited clinical efficacy without reconstruction of the NP. On the other hand, transplants into the substantia nigra in the mesencephalon do not project as to reach their target at the dorsolateral striatum [45], or do so to a limited extent when homotopic transplants are held [46, 47], or when transplant consist of simultaneous grafts of neurons into the striatum and the substantia nigra [45]. Reconstruction of the NP however, allowed the restoration of complex sensory-motor behaviors in hemiparkinsonian rats [45–48]. An important observation is that axon regeneration and outgrowth in the CNS is better in developing and neonatal neural tissue than in adult tissue. Reconstruction of the NP by nigral grafts implanted into the ventral mesencephalon of neonatal rats has been demonstrated as compared with adult rats [49, 50], supporting the idea that a more permissive environment is present in younger animals. In the adults, CNS myelin associated proteins can inhibit axonal outgrowth after an injury; nevertheless neutralization of the proteins by antibodies, or knock-out mice for myelin associated proteins or their receptors failed to enhance regeneration or did so to a limited extent [51–53]; suggesting that additional factors, or the lack of them are impairing the outgrowth. Extracellular matrices, proteoglycans and other guidance cues like chemotropic proteins are involved in NP pathway formation [54], and could have an important role during axon projection and regeneration. Glial cell line derived neurotrophic factor (GDNF) for example has a role in mDA axon growth [55], its mRNA is differentially expressed in striatal dopaminergic areas in developing and neonatal tissue versus adult tissue [56], and their use in intranigral transplanted animals with fetal ventral mescencephalic grafts improved axon outgrowth [57]. Therefore, for a successful cell replacement therapy, it is desirable to have a permissive extracellular environment that promotes axon projection, the correct innervation of normal striatal targets and reconstruction of the NP. The enhancement by sema 3A and 3C of axonal outgrowth and

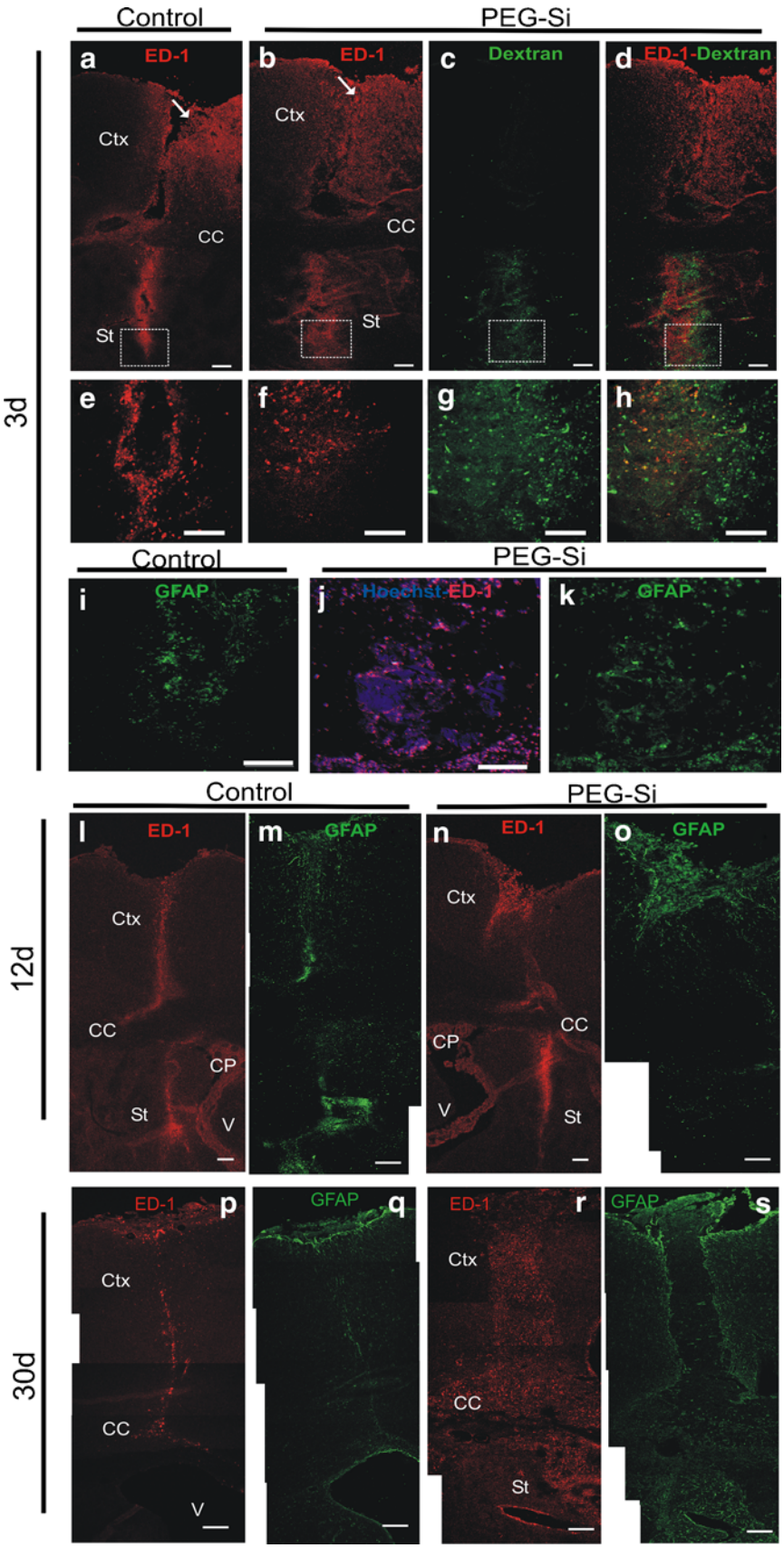

Fig. 5 Biocompatibility of PEG-Si nano-gel after injection into the striatum. Confocal microscopy reconstructed images of tissue sections of saline solution (control) (**a**, **e**, **i**, **l**, **m**, **p**, **q**) or PEG-Si gel (**b**–**d**, **f**–**h**, **j**, **k**, **n**, **o**, **r**, **s**) implanted striatum, obtained at 3 (**a**–**k**), 12 (**l**–**o**), or 30 days (**p**–**s**) after injection. Coronal sections were immunostained with ED-1 antibody to identify activated macrophages or with GFAP to identify glial cells. *Dotted line squares* in **a**–**d** indicate the area magnified in **e**–**h**. (**c**, **d**) Images showing the fluorescent signal of the FITC-dextran loaded gel at the striatum (St), and the presence of some macrophages at the dextran loaded gel, (magnified in **h**), or Hoechst loaded gel (**j**) (*blue*). (**i**, **k**) A similar recruitment of GFAP positive cells is observed in the deepest point of the injection site after 3 days of injection. *CC* corpus callosum, *Ctx* cortex, *CP* choroid plexus, *St* striatum, *V* ventricle. *Scale bars* 100 μm

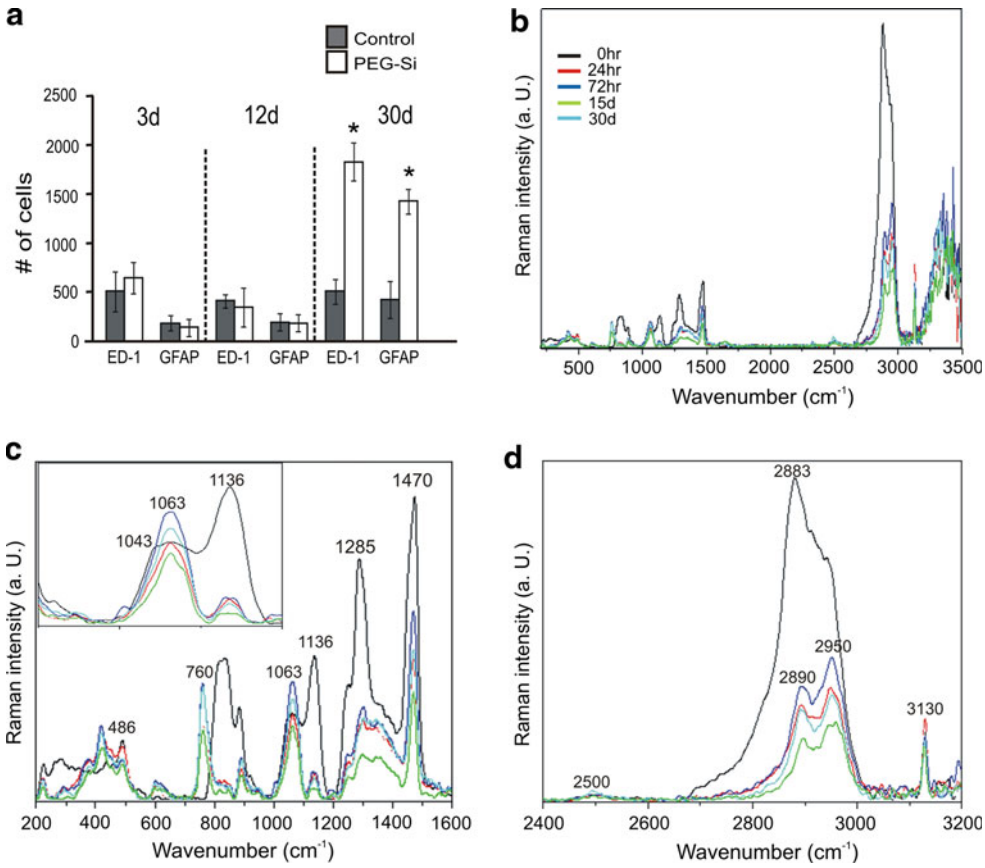

Fig. 6 Quantification of ED-1 and GFAP positive cells at injury site and biodegradation of PEG-Si. **a** Quantification of ED1- or GFAP-positive cells in selected serial sections of saline solution (control) or PEG-Si gel implanted striatum at different days post injection. An increase in ED1 and GFAP cells in PEG-Si gel treated samples as compared with control samples was observed after 30 days, (*$P < 0.05$, according to Student's *t*-test) (3 days, $n = 4$ rats; 12 and 30 days, $n = 3$ rats). **b–d** Scattered Raman spectroscopy of PEG-Si gel incubated for different periods of time in SBF. Code *color* in **b** applies to **c** and **d**

attraction of mDA neurons, including those derived from differentiated embryonic stem cells have opened the possibility of using these molecules in cell replacement therapies to guide the axons to their correct targets [29]. Delivery of sema 3A and 3C from transfected cells in hemiparkinsonian rats transplanted with DA neurons differentiated from embryonic stem cells led to axonal projections to the striatum, behavioral improvement, and dopamine release in rats, as compared to intranigral transplants without semaphorin expressing cells (unpublished results). These promising results indicate that semaphorins are useful complements to cell replacement therapies. The use of a transfected cell line to deliver semaphorins however, is not a suitable method for delivery of semaphorins, since they could lead to immune response, uncontrolled growth, and the consequent tumor formation.

The experiments in the present report are the first attempt to use a nanostructured biomaterial as injectable depots to establish a semaphorin gradient and to direct axonal growth of DA neurons with potential use in regenerative therapy for PD. The thixotropic formulation used provides the benefit of avoiding the need for chemical or photocrosslinking reactions in order to form the gel, as the polymerization initiators for the latter processes may have detrimental effects on viability of cells and proteins. The thixotropic, injectable system is further advantageous as it is a low invasive method for introducing a hydrogel depot into the desired region. Furthermore, the fast setting properties of the gel (<1 min) prevents it from leaking into the surrounding tissue and the diffusion of the protein out of the depot and into the collagen gel leads to the formation of a defined protein gradient. The value of PEG-Si nano-gel for semaphorin delivery is also reflected in the in vitro experiments where cells were either immobilized on laminin (for DRG neurons) or within a collagen gel (for dopaminergic neurons) and pronounced growth cone collapse or axonal outgrowth responses were observed in the DRG and dopaminergic neurons respectively. Although no cytotoxic effect was observed when the neurons were exposed to the PEG-Si nano-gel for several days in culture, and no early immune response to PEG-Si nano-gel was observed in the in vivo implantation experiments, evidence of a late-onset immune response in the long-term gel implants was observed. In vitro experiments showed degradation of PEG, while no evidence of degradation of silica particles was obtained; suggesting that the latter could be inducing the inflammatory response.

The biocompatibility of silica nanoparticles is still under study and the literature reports evidences of both biocompatible and non-biocompatible characteristics. There are

reports of a fast and safe clearance of silica nanoparticles from the animal body through renal excretion [58–60]. Single and repeated dose of mesoporous silica nanoparticles under 80 mg/kg cause no toxicity after intravenous injection in mice, while higher doses cause toxicity [61]. Moreover, the presence of silica in nanocomposites of poly-2-hydroxyethylmethacrylate (pHEMA) or poly (ε-caprolactone) (PCL) improves cell attachment and differentiation, without cytotoxic effects [62, 63], and mesosporous silica nanoparticles did not impair macrophage phagocytosis nor did it affect macrophage secretion of cytokines [64, 65]. On the other hand however; silica particles activate the NLRP3 receptor in macrophages, also called the inflammasome, inducing lysosomal rupture and activating highly inflammatory cytokines [66]. It has also been reported that nanosized mesoporous particles affect viability of in vitro human dendritic cells and the expression of immune markers, as compared with microsized silica particles [67]. It is important to mention that the effects of silica nanoparticles in cell apoptosis, uptake and migration depends on several factors like the shape of the particles [68], the size, and the concentration [67], and therefore the biocompatibility must be assayed for each particular case. Moreover, the compatibility of amorphous silica nanoparticles can be improved by coating the particles with the surfactant PluronicF127, these results were directly related to the amount of protein adsorption to the surface of uncoated particles [69]. PEG also reduces protein adsorption on the surface of silica nanoparticles, a key factor that reduces immunogenicity and improves biocompatibility [70, 71]. The comprehension of the factors that modify the compatibility of silica nanoparticles and nanostructured biomaterials containing silica particles, however, is incomplete, and many studies are needed to improve the current knowledge; especially needed are more long term, in vivo studies involving the use of immunocompetent cells.

An aspect that has to be pursued in more detail regarding the use of biomaterials for delivery of proteins in the brain is the development of low viscosity formulations; this would allow the use of finer cannulae for the implantation procedures. As shown in previous studies, the local trauma after the transplantation procedure is a determinant factor for graft survival and for the lymphocytes and glia reactions [34, 72–74], and reduction of this trauma could avoid an extended and deleterious inflammation. Overall, our results revealed a good in vitro performance of PEG-Si nano-gel for the controlled delivery of proteins with chemotropic properties upon growing axons. Long term in vivo implantation, however, could lead to undesirable effects at the lesion site. A detailed characterization of the effects of delivery vehicles in the brain has to be done to design the most suitable option to deliver proteins such as semaphorins and to improve in vivo axonal outgrowth in neuronal transplantation procedures.

Acknowledgments We thank to Fabian Diaz, Emmanuel Diaz-Martinez, Soledad Mendoza, Elsa Nydia Hernández, and Martín García-Servín for their technical support. We also thank Dororthy Pless for editing the manuscript style. This work was supported by National Council of Science and Technology of Mexico (CONACYT), grant number 82482; and National University of México (UNAM), grant DGAPA-UNAM IN217810-21 and IMPULSA02-UNAM (stem cell group).

Disclosure Authors declare no conflict of interest.

References

1. Check E. Harmful potential of viral vectors fuels doubts over gene therapy. Nature. 2003;423:573–4.
2. Sawyer AJ, Piepmeier JM, Saltzman WM. New methods for direct delivery of chemotherapy for treating brain tumors. Yale J Biol Med. 2006;79:141–52.
3. Morris MI, Fischer SA, Ison MG. Infections transmitted by transplantation. Infect Dis Clin North Am. 2010;24:497–514.
4. McRae A, Hjorth S, Mason DW, Dillon L, Tice TR. Microencapsulated dopamine (DA)-induced restitution of function in 6-OHDA-denervated rat striatum in vivo: comparison between two microsphere excipients. J Neural Transplant Plast. 1991;2:165–73.
5. Maysinger D, Jalsenjak I, Cuello AC. Microencapsulated nerve growth factor: effects on the forebrain neurons following devascularizing cortical lesions. Neurosci Lett. 1992;140:71–4.
6. Klose D, Siepmann F, Willart JF, Descamps M, Siepmann J. Drug release from PLGA-based microparticles: effects of the "microparticle:bulk fluid" ratio. Int J Pharm. 2009;383:123–31.
7. Nkansah MK, Tzeng SY, Holdt AM, Lavik EB. Poly(lactic-co-glycolic acid) nanospheres and microspheres for short- and long-term delivery of bioactive ciliary neurotrophic factor. Biotechnol Bioeng. 2008;100:1010–9.
8. Burdick JA, Ward M, Liang E, Young MJ, Langer R. Stimulation of neurite outgrowth by neurotrophins delivered from degradable hydrogels. Biomaterials. 2006;27:452–9.
9. Jain A, Kim YT, McKeon RJ, Bellamkonda RV. In situ gelling hydrogels for conformal repair of spinal cord defects, and local delivery of BDNF after spinal cord injury. Biomaterials. 2006;27:497–504.
10. Piantino J, Burdick JA, Goldberg D, Langer R, Benowitz LI. An injectable, biodegradable hydrogel for trophic factor delivery enhances axonal rewiring and improves performance after spinal cord injury. Exp Neurol. 2006;201:359–67.
11. Jhaveri SJ, Hynd MR, Dowell-Mesfin N, Turner JN, Shain W, Ober CK. Release of nerve growth factor from HEMA hydrogel-coated substrates and its effect on the differentiation of neural cells. Biomacromolecules. 2009;10:174–83.
12. Lee K, Silva EA, Mooney DJ. Growth factor delivery-based tissue engineering: general approaches and a review of recent developments. J R Soc Interface. 2011;8:153–70.
13. Bagnard D, Lohrum M, Uziel D, Puschel AW, Bolz J. Semaphorins act as attractive and repulsive guidance signals during the development of cortical projections. Development. 1998;125:5043–53.
14. Bagnard D, Thomasset N, Lohrum M, Puschel AW, Bolz J. Spatial distributions of guidance molecules regulate chemorepulsion and chemoattraction of growth cones. J Neurosci. 2000;20:1030–5.

15. Rosentreter SM, Davenport RW, Loschinger J, Huf J, Jung J, Bonhoeffer F. Response of retinal ganglion cell axons to striped linear gradients of repellent guidance molecules. J Neurobiol. 1998;37:541–62.
16. Isbister CM, Mackenzie PJ, To KC, O'Connor TP. Gradient steepness influences the pathfinding decisions of neuronal growth cones in vivo. J Neurosci. 2003;23:193–202.
17. Unified nomenclature for the semaphorins/collapsins. Semaphorin Nomenclature Committee. Cell. 1999;97:551–52.
18. Tessier-Lavigne M, Goodman CS. The molecular biology of axon guidance. Science. 1996;274:1123–33.
19. Messersmith EK, Leonardo ED, Shatz CJ, Tessier-Lavigne M, Goodman CS, Kolodkin AL. Semaphorin III can function as a selective chemorepellent to pattern sensory projections in the spinal cord. Neuron. 1995;14:949–59.
20. Moreno-Flores MT, Martin-Aparicio E, Martin-Bermejo MJ, Agudo M, McMahon S, Avila J, Diaz-Nido J, Wandosell F. Semaphorin 3C preserves survival and induces neuritogenesis of cerebellar granule neurons in culture. J Neurochem. 2003;87:879–90.
21. Polleux F, Morrow T, Ghosh A. Semaphorin 3A is a chemoattractant for cortical apical dendrites. Nature. 2000;404:567–73.
22. Hernandez-Montiel HL, Tamariz E, Sandoval-Minero MT, Varela-Echavarria A. Semaphorins 3A, 3C, and 3F in mesencephalic dopaminergic axon pathfinding. J Comp Neurol. 2008;506:387–97.
23. Mann F, Chauvet S, Rougon G. Semaphorins in development and adult brain: implication for neurological diseases. Prog Neurobiol. 2007;82:57–79.
24. Song H, Ming G, He Z, Lehmann M, McKerracher L, Tessier-Lavigne M, Poo M. Conversion of neuronal growth cone responses from repulsion to attraction by cyclic nucleotides. Science. 1998;281:1515–8.
25. Terman JR, Kolodkin AL. Nervy links protein kinase a to plexin-mediated semaphorin repulsion. Science. 2004;303:1204–7.
26. Castellani V, De Angelis E, Kenwrick S, Rougon G. Cis and trans interactions of L1 with neuropilin-1 control axonal responses to semaphorin 3A. EMBO J. 2002;21:6348–57.
27. Falk J, Bechara A, Fiore R, Nawabi H, Zhou H, Hoyo-Becerra C, Bozon M, Rougon G, Grumet M, Puschel AW, Sanes JR, Castellani V. Dual functional activity of semaphorin 3B is required for positioning the anterior commissure. Neuron. 2005;48:63–75.
28. Schlomann U, Schwamborn JC, Muller M, Fassler R, Puschel AW. The stimulation of dendrite growth by Sema3A requires integrin engagement and focal adhesion kinase. J Cell Sci. 2009;122:2034–42.
29. Tamariz E, Diaz-Martinez NE, Diaz NF, Garcia-Pena CM, Velasco I, Varela-Echavarria A. Axon responses of embryonic stem cell-derived dopaminergic neurons to semaphorins 3A and 3C. J Neurosci Res. 2010;88:971–80.
30. Kim JH, Auerbach JM, Rodriguez-Gomez JA, Velasco I, Gavin D, Lumelsky N, Lee SH, Nguyen J, Sanchez-Pernaute R, Bankiewicz K, McKay R. Dopamine neurons derived from embryonic stem cells function in an animal model of Parkinson's disease. Nature. 2002;418:50–6.
31. Lee SH, Lumelsky N, Studer L, Auerbach JM, McKay RD. Efficient generation of midbrain and hindbrain neurons from mouse embryonic stem cells. Nat Biotechnol. 2000;18:675–9.
32. Soldner F, Hockemeyer D, Beard C, Gao Q, Bell GW, Cook EG, Hargus G, Blak A, Cooper O, Mitalipova M, Isacson O, Jaenisch R. Parkinson's disease patient-derived induced pluripotent stem cells free of viral reprogramming factors. Cell. 2009;136:964–77.
33. Wernig M, Zhao JP, Pruszak J, Hedlund E, Fu D, Soldner F, Broccoli V, Constantine-Paton M, Isacson O, Jaenisch R. Neurons derived from reprogrammed fibroblasts functionally integrate into the fetal brain and improve symptoms of rats with Parkinson's disease. Proc Natl Acad Sci USA. 2008;105:5856–61.
34. Bjorklund A, Stenevi U, Schmidt RH, Dunnett SB, Gage FH. Intracerebral grafting of neuronal cell suspensions. II. Survival and growth of nigral cell suspensions implanted in different brain sites. Acta Physiol Scand Suppl. 1983;522:9–18.
35. Isacson O, Bjorklund LM, Schumacher JM. Toward full restoration of synaptic and terminal function of the dopaminergic system in Parkinson's disease by stem cells. Ann Neurol. 2003;53(Suppl 3):S135–46.
36. Pek YS, Wan AC, Shekaran A, Zhuo L, Ying JY. A thixotropic nanocomposite gel for three-dimensional cell culture. Nat Nanotechnol. 2008;3:671–5.
37. Kolodkin AL, Levengood DV, Rowe EG, Tai YT, Giger RJ, Ginty DD. Neuropilin is a semaphorin III receptor. Cell. 1997;90:753–62.
38. Diaz NF, Guerra-Arraiza C, Diaz-Martinez NE, Salazar P, Molina-Hernandez A, Camacho-Arroyo I, Velasco I. Changes in the content of estrogen alpha and progesterone receptors during differentiation of mouse embryonic stem cells to dopamine neurons. Brain Res Bull. 2007;73:75–80.
39. Kokubo T, Kushitani H, Sakka S, Kitsugi T, Yamamuro T. Solutions able to reproduce in vivo surface-structure changes in bioactive glass-ceramic A-W. J Biomed Mater Res. 1990;24:721–34.
40. Luo Y, Raible D, Raper JA. Collapsin: a protein in brain that induces the collapse and paralysis of neuronal growth cones. Cell. 1993;75:217–27.
41. Dupeyron D, Rieumont J, González M, Castaño VM. Protein delivery by enteric copolymer nanoparticles. J Dispers Sci Technol. 2009;30:1–7.
42. Colthup BN, Daly HL, Wiberley ES. Introduction to infrared and Raman spectroscopy. 3rd ed. San Diego: Academic Press; 1990.
43. Nakamoto K. Infrared and Raman spectra of inorganic and coordination compounds. 3rd ed. New York: Wiley; 1978.
44. Hargus G, Cooper O, Deleidi M, Levy A, Lee K, Marlow E, Yow A, Soldner F, Hockemeyer D, Hallett PJ, Osborn T, Jaenisch R, Isacson O. Differentiated Parkinson patient-derived induced pluripotent stem cells grow in the adult rodent brain and reduce motor asymmetry in Parkinsonian rats. Proc Natl Acad Sci USA. 2010;107:15921–6.
45. Mendez I, Sadi D, Hong M. Reconstruction of the nigrostriatal pathway by simultaneous intrastriatal and intranigral dopaminergic transplants. J Neurosci. 1996;16:7216–27.
46. Thompson LH, Grealish S, Kirik D, Bjorklund A. Reconstruction of the nigrostriatal dopamine pathway in the adult mouse brain. Eur J Neurosci. 2009;30:625–38.
47. Gaillard A, Decressac M, Frappe I, Fernagut PO, Prestoz L, Besnard S, Jaber M. Anatomical and functional reconstruction of the nigrostriatal pathway by intranigral transplants. Neurobiol Dis. 2009;35:477–88.
48. Baker KA, Sadi D, Hong M, Mendez I. Simultaneous intrastriatal and intranigral dopaminergic grafts in the parkinsonian rat model: role of the intranigral graft. J Comp Neurol. 2000;426:106–16.
49. Nikkhah G, Cunningham MG, Cenci MA, McKay RD, Bjorklund A. Dopaminergic microtransplants into the substantia nigra of neonatal rats with bilateral 6-OHDA lesions. I. Evidence for anatomical reconstruction of the nigrostriatal pathway. J Neurosci. 1995;15:3548–61.
50. Nikkhah G, Cunningham MG, McKay R, Bjorklund A. Dopaminergic microtransplants into the substantia nigra of neonatal rats with bilateral 6-OHDA lesions. II. Transplant-induced behavioral recovery. J Neurosci. 1995;15:3562–70.
51. Lee JK, Geoffroy CG, Chan AF, Tolentino KE, Crawford MJ, Leal MA, Kang B, Zheng B. Assessing spinal axon regeneration and sprouting in Nogo-, MAG-, and OMgp-deficient mice. Neuron. 2010;66:663–70.

52. Omoto S, Ueno M, Mochio S, Takai T, Yamashita T. Genetic deletion of paired immunoglobulin-like receptor B does not promote axonal plasticity or functional recovery after traumatic brain injury. J Neurosci. 2010;30:13045–52.
53. Nakamura Y, Fujita Y, Ueno M, Takai T, Yamashita T. Paired immunoglobulin-like receptor B knockout does not enhance axonal regeneration or locomotor recovery after spinal cord injury. J Biol Chem. 2011;286:1876–83.
54. Van den Heuvel DM, Pasterkamp RJ. Getting connected in the dopamine system. Prog Neurobiol. 2008;85:75–93.
55. Krieglstein K. Factors promoting survival of mesencephalic dopaminergic neurons. Cell Tissue Res. 2004;318:73–80.
56. Stromberg I, Bjorklund L, Johansson M, Tomac A, Collins F, Olson L, Hoffer B, Humpel C. Glial cell line-derived neurotrophic factor is expressed in the developing but not adult striatum and stimulates developing dopamine neurons in vivo. Exp Neurol. 1993;124:401–12.
57. Tang FI, Tien LT, Zhou FC, Hoffer BJ, Wang Y. Intranigral ventral mesencephalic grafts and nigrostriatal injections of glial cell line-derived neurotrophic factor restore dopamine release in the striatum of 6-hydroxydopamine-lesioned rats. Exp Brain Res. 1998;119:287–96.
58. Lu J, Liong M, Li Z, Zink JI, Tamanoi F. Biocompatibility, biodistribution, and drug-delivery efficiency of mesoporous silica nanoparticles for cancer therapy in animals. Small. 2010;6:1794–805.
59. He X, Nie H, Wang K, Tan W, Wu X, Zhang P. In vivo study of biodistribution and urinary excretion of surface-modified silica nanoparticles. Anal Chem. 2008;80:9597–603.
60. Burns AA, Vider J, Ow H, Herz E, Penate-Medina O, Baumgart M, Larson SM, Wiesner U, Bradbury M. Fluorescent silica nanoparticles with efficient urinary excretion for nanomedicine. Nano Lett. 2009;9:442–8.
61. Hudson SP, Padera RF, Langer R, Kohane DS. The biocompatibility of mesoporous silicates. Biomaterials. 2008;29:4045–55.
62. Calandrelli L, Annunziata M, Della Ragione F, Laurienzo P, Malinconico M, Oliva A. Development and performance analysis of PCL/silica nanocomposites for bone regeneration. J Mater Sci Mater Med. 2010;21:2923–36.
63. D'Agostino A, Errico ME, Malinconico M, De Rosa M, Avella M, Schiraldi C. Development of nanocomposite based on hydroxyethylmethacrylate and functionalized fumed silica: mechanical, chemico-physical and biological characterization. J Mater Sci Mater Med. 2011;22:481–90.
64. Witasp E, Kupferschmidt N, Bengtsson L, Hultenby K, Smedman C, Paulie S, Garcia-Bennett AE, Fadeel B. Efficient internalization of mesoporous silica particles of different sizes by primary human macrophages without impairment of macrophage clearance of apoptotic or antibody-opsonized target cells. Toxicol Appl Pharmacol. 2009;239:306–19.
65. Kunzmann A, Andersson B, Thurnherr T, Krug H, Scheynius A, Fadeel B. Toxicology of engineered nanomaterials: focus on biocompatibility, biodistribution and biodegradation. Biochim Biophys Acta. 2010;1810:361–73.
66. Hornung V, Bauernfeind F, Halle A, Samstad EO, Kono H, Rock KL, Fitzgerald KA, Latz E. Silica crystals and aluminum salts activate the NALP3 inflammasome through phagosomal destabilization. Nat Immunol. 2008;9:847–56.
67. Vallhov H, Gabrielsson S, Stromme M, Scheynius A, Garcia-Bennett AE. Mesoporous silica particles induce size dependent effects on human dendritic cells. Nano Lett. 2007;7:3576–82.
68. Huang X, Teng X, Chen D, Tang F, He J. The effect of the shape of mesoporous silica nanoparticles on cellular uptake and cell function. Biomaterials. 2010;31:438–48.
69. Dutta D, Sundaram SK, Teeguarden JG, Riley BJ, Fifield LS, Jacobs JM, Addleman SR, Kaysen GA, Moudgil BM, Weber TJ. Adsorbed proteins influence the biological activity and molecular targeting of nanomaterials. Toxicol Sci. 2007;100:303–15.
70. Cauda V, Schlossbauer A, Bein T. Bio-degradation study of colloidal mesoporous silica nanoparticles: effect of surface functionalization with organo-silanes and poly(ethylene glycol). Microp Mesop Mater. 2010;132:60–71.
71. Xu H, Yan F, Monson EE, Kopelman R. Room-temperature preparation and characterization of poly (ethylene glycol)-coated silica nanoparticles for biomedical applications. J Biomed Mater Res. 2003;A 66:870–9.
72. Nikkhah G, Olsson M, Eberhard J, Bentlage C, Cunningham MG, Bjorklund A. A microtransplantation approach for cell suspension grafting in the rat Parkinson model: a detailed account of the methodology. Neuroscience. 1994;63:57–72.
73. Olanow CW. Surgical therapy for Parkinson's disease. Eur J Neurol. 2002;9(Suppl 3):31–9.
74. Steiner B, Winter C, Blumensath S, Paul G, Harnack D, Nikkhah G, Kupsch A. Survival and functional recovery of transplanted human dopaminergic neurons into hemiparkinsonian rats depend on the cannula size of the implantation instrument. J Neurosci Methods. 2008;169:128–34.